Oxygen Activation

DOI: 10.1002/anie.201402783

# Superoxide Formation on Isolated Cationic Gold Clusters**

*Alex P. Woodham and André Fielicke**

***Abstract:*** *Gold nanoparticles are known to be highly versatile oxidation catalysts utilizing molecular oxygen as a feedstock, but the mechanism and species responsible for activating oxygen remain unclear. The reaction between unsupported cationic gold clusters and molecular oxygen has been investigated. The resulting complexes were characterized in the gas phase using IR spectroscopy. A strong red-shift in the observed ν(O-O) stretching frequency indicates the formation of superoxo ($O_2^-$) moieties. These moieties are seen to form spontaneously in systems, which upon electron transfer attain a closed shell within the spherical jellium model ($Au_{10}^+$ and $Au_{22}^+$), whereas an oxygen induced self-promotion in the activation is observed for other systems ($Au_4^+$, $Au_{12}^+$, $Au_{21}^+$).*

Gold nanoparticles show the surprising ability to catalyze a range of oxidation reactions under extremely mild conditions, utilizing molecular oxygen as a feedstock and often with a high degree of selectivity.[1] The mechanism behind the reactions remains a mystery despite their extensive investigation. Even in one of the simplest cases, the oxidation of carbon monoxide, the nature of the active site is much debated.[2] It is generally accepted that the CO adsorbs to the gold nanoparticle but the mechanism for activation of oxygen remains unclear. Proposals vary from the importance of the three-phase boundary between the gold cluster, supporting surface and reagent phase[3] to the gold particle interacting with regions of excess electron density,[4] thereby acquiring a partial negative charge and enabling it to activate oxygen itself. Yet other investigations reveal the importance of positively charged gold centers for the observed activity.[5]

To obtain an experimental handle on these complex systems, one possible approach is to simplify the problem by introducing the clusters into the gas phase. These studies have demonstrated that neutral and negatively charged gold clusters interact with $O_2$ to form activated superoxo ($O_2^-$) moieties.[6] Furthermore, reaction kinetics have been observed for $Au_2^-$ that are consistent with a catalytic cycle for the oxidation of CO by $O_2$.[7] The cationic clusters, meanwhile, are reported to only react with oxygen in the presence of electron donating promoters (for example, $N_2$ or $H_2$[8]), with the exception of $Au_{10}^+$.[9] This is in clear contradiction to the results from the surface science community.[5]

Herein we demonstrate the formation of cationic gold cluster oxygen complexes and characterize them by IR spectroscopy in the frequency range corresponding to the internal O–O stretch vibrations. This vibrational mode is inherently sensitive on the electronic occupation of the $O_2$ π* (anti-bonding) highest occupied molecular orbital (HOMO). Changes in this vibrational frequency reflect changes in the $O_2$ oxidation state. The recorded spectra unequivocally demonstrate the formation of activated oxygen species without the need for a support interaction or the presence of a promoting ligand, casting light on the mechanism of this fundamental reaction. We also present evidence of self-promoted activation in conditions where multiple ligands are complexed with the gold cluster.

The cationic clusters are formed by laser ablation of a solid gold target and quenching of the plasma by a short helium pulse. After thermalization to −60 °C within a reaction channel downstream from the cluster source, a pulse of oxygen is introduced. The total pressure in the channel is estimated to be about 20 mbar and the partial pressure of $O_2$ will be a few mbar. The reaction time is given by the flow time through the channel, which is about 100 μs. Complex formation is stopped by expansion into the vacuum and formation of a molecular beam. The distribution of cationic cluster species is analyzed by time-of-flight mass spectrometry. Vibrational spectra specific for all species are obtained by mass-resolved IR multiple photon dissociation (IR-MPD) spectroscopy. For this, the cluster beam is overlapped by the pulsed infrared beam from the free electron laser for IR experiments (FELIX).[10] If the IR light is in resonance with a vibrational mode of the complex, sequential pumping of this mode and internal vibrational redistribution results in a heating of the cluster, leading to fragmentation. Monitoring the complex signal intensity as a function of IR wavelength allows for dissociation spectra to be recorded.[11]

Figure 1 gives the dissociation spectra recorded in the $Au_{10}O_2^+$, $Au_{10}(O_2)_2^+$, and $Au_{22}O_2^+$ mass channels. The reported spectra are deconvoluted from the raw data such that the effects of a cluster fragmenting into a lower coverage complex are accounted for. The most prominent feature in all three spectra is around 1065 $cm^{-1}$, consistent with the presence of a superoxo moiety.[12] An additional, weaker feature is seen for $Au_{10}(O_2)_2^+$ at 1523 $cm^{-1}$ and corresponds to the presence of a physisorbed dioxygen ligand, indicating that it is simply a spectator species to the cluster complex. This is

[*] A. P. Woodham, Dr. A. Fielicke
Institut für Optik und Atomare Physik
Technische Universität Berlin
Hardenbergstrasse 36, 10623 Berlin (Germany)
E-mail: fielicke@physik.tu-berlin.de

[**] We gratefully acknowledge the support of the Stichting voor Fundamenteel Onderzoek der Materie (FOM) for providing beam time on FELIX, and the FELIX staff for their skilful assistance, in particular Dr. B. Redlich and Dr. A. F. G. van der Meer. This work is supported by the Fritz-Haber Institute of the Max-Planck Society, the Cluster of Excellence "Unifying Concepts in Catalysis" coordinated by the Technical University Berlin and funded by the Deutsche Forschungsgemeinschaft (DFG), and through the DFG within the research unit FOR 1282 (FI 893/4). We thank Dr. C. Kerpal for implementation of the modified basin hopping algorithm.

Supporting information for this article is available on the WWW under http://dx.doi.org/10.1002/anie.201402783.

  

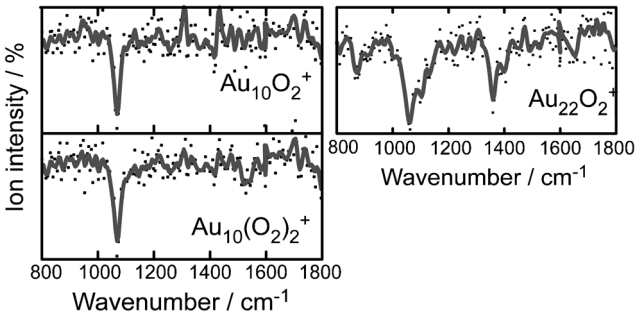


***Figure 1.*** IR-MPD spectra recorded for $Au_{10}O_2^+$, $Au_{10}(O_2)_2^+$, and $Au_{22}O_2^+$ in the range of the O–O stretching vibrations. The dots are the raw data points, corresponding to an average of about 400 single measurements; the lines are their five-point binomially weighted running average. The most intense peaks correspond to depletion to about 20% of the initial intensity.

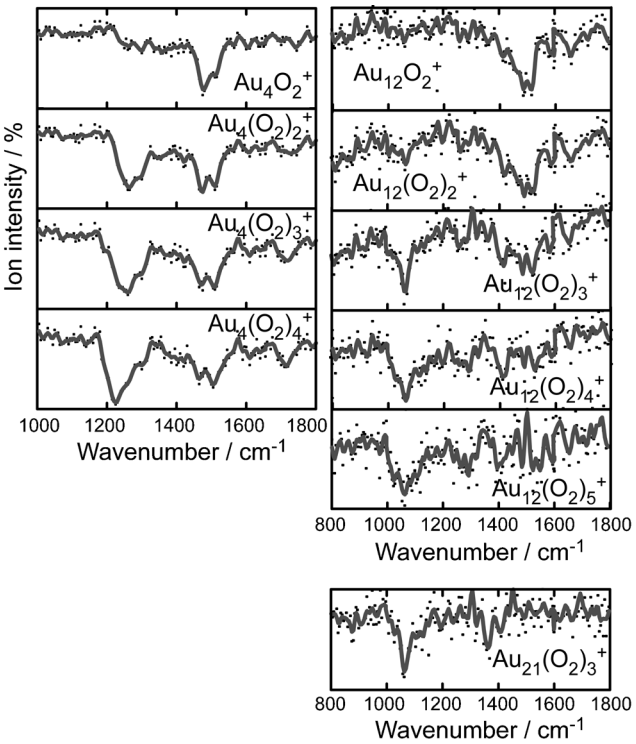


***Figure 2.*** IR-MPD spectra recorded for $Au_4(O_2)_m^+$, $Au_{12}(O_2)_m^+$, and $Au_{21}(O_2)_3^+$. These clusters only demonstrate a superoxo-like mode when multiple oxygen ligands are complexed with the cluster.

true for all of the higher coverage complexes ($Au_{10}(O_2)_m^+$, $m = 3$–6; not shown). The spectrum for $Au_{22}O_2^+$ is significantly more complex, with two satellite features being present. One of these is red-shifted to 875 cm$^{-1}$ whilst the second is blue-shifted to around 1359 cm$^{-1}$. The band positions have estimated uncertainties of $\pm 5$ cm$^{-1}$, given by the bandwidth of the laser and the uncertainty of the laser calibration. These additional modes are either an indication of isomerism in the oxygen binding location[6a,b,13] or are due to combination/difference bands with other vibrational modes. The absorption in $Au_{22}O_2^+$ is also broader than for $Au_{10}O_2^+$, again suggesting isomerism. All experiments have been repeated with $^{18}O_2$ and show shifts consistent with the observation of dioxygen-related vibrations (example spectra for $Au_4(^{18}O_2)_m^+$ are shown in the Supporting Information, Figure S1).

Along with these species, oxygen complexes are also observed for all of the smaller cationic gold clusters ($Au_nO_2^+$; $n = 2$–12), with $Au_{10}O_2^+$ being a maximum in the reactivity. The reactivity drops off rapidly after $Au_{10}O_2^+$, but with conditions optimized for the production of larger cluster complexes, species as large as $Au_{24}O_2^+$ are observed (see the Supporting Information, Figure S2 for a mass spectrum).

Figure 2 gives the IR-MPD spectra recorded in the $Au_4(O_2)_m^+$, $Au_{12}(O_2)_m^+$, and $Au_{21}(O_2)_3^+$ mass channels. Unlike $Au_{10}^+$ and $Au_{22}^+$, the superoxo mode is not observed for the species containing a single oxygen ligand. Instead it is seen to be dependent upon the number of ligands complexed with the gold cluster. For $Au_{21}(O_2)_{1\text{-}2}^+$, no bands are seen, indicating either a dissociative adsorption or a sufficiently weakly interacting physisorbed complex such that the formally IR-inactive O–O stretch is not observed. With the addition of the third oxygen, however, two modes appear, one at 1063 cm$^{-1}$, characteristic for a superoxide, and a second, blue-shifted at 1363 cm$^{-1}$. The $Au_{12}O_2^+$ complex shows a single band consistent with a physisorbed dioxygen moiety. With increasing oxygen coverage the intensity of this feature decreases whilst a second feature at 1063 cm$^{-1}$ grows in. Finally for $Au_4(O_2)_m^+$ only a single feature at 1470 cm$^{-1}$ is observed for the $m = 1$ case whilst for $m \geq 2$ a new mode is observed at 1260 cm$^{-1}$, which red-shifts with oxygen coverage towards 1240 cm$^{-1}$. Such frequencies are halfway between the frequency of a superoxo moiety and the stretching frequency of the physisorbed complex. With increasing oxygen coverage, the physisorbed mode is seen to split into two features separated by about 30–40 cm$^{-1}$, although this may be an experimental artefact. A third feature is also present in the $Au_4(O_2)_m^+$ spectra, at $1720 \pm 10$ cm$^{-1}$. This absorption is clearly present for $m = 3$ and 4 and potentially also for $m = 1$ and 2. Such a frequency could correspond to the formation of a dioxygenyl moiety ($O_2^+$) or be a combination band of the physisorbed mode and an internal mode.

The bands at 1063 cm$^{-1}$ are characteristic for the superoxo ligand and confirm the presence of the same activated dioxygen species as identified for $O_2$ bound to neutral and anionic gold clusters.[6a,b] This is surprising given the formally required electron removal from the gold cluster to form the superoxide, which should be energetically unfavorable for an already positively charged cluster. Even for anionic gold clusters, such electron transfer is only possible for the even-sized, open-shell clusters that have a sufficiently low electron affinity.[6a,c,d,14] The neutral clusters show a reversed pattern, with only certain odd-sized clusters forming the superoxo species. With the driving force appearing to be the formation of an ion–ion complex and a further stabilization of the now cationic cluster core by structural rearrangement.[6b] Such a reaction, however, has been speculated to occur in cationic silver clusters.[15]

To obtain more insights into the mechanism of $O_2$ activation at the cationic gold clusters, supporting quantum

  

chemical calculations using density functional theory (DFT) were performed (for details, see the Supporting Information). Owing to the increase in complexity and configuration space as the cluster system increases in size, we have limited these investigations to $Au_4O_2^+$, $Au_4(O_2)_2^+$, and $Au_{10}O_2^+$ only. The predicted structures for these complexes are given in Figure 3.

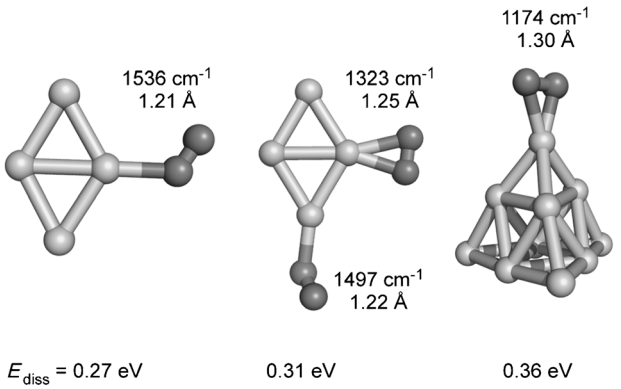


***Figure 3.*** Structures for $Au_4(O_2)^+$, $Au_4(O_2)_2^+$, and $Au_{10}O_2^+$. The structure for $Au_{10}O_2^+$ was obtained from a basin-hoping global optimization algorithm with the constraint that the oxygen molecule was not allowed to dissociate; otherwise atoms were free to move independently. The calculated oxygen stretching frequencies, O–O bond lengths, and oxygen binding energies (ZPE corrected) are given. For $Au_4(O_2)_2^+$, the binding energy is for the second dioxygen molecule.

Species containing weakly physisorbed oxygen are known to be difficult for DFT to accurately reproduce,[16] often suffering from spin-contamination effects. As such the assigned structures are the lowest energy species found which are not significantly affected by spin contamination. In cases where electron transfer occurs, that is, when the spins are strongly coupled, this is seen to be a minor problem. The O–O stretching frequencies agree qualitatively with the experiment. The structures for $Au_4O_2^+$ and $Au_4(O_2)_2^+$ are based on the known structure for bare $Au_4^+$,[17] with the first oxygen moiety predicted to be bound by 0.26 eV to one of the three-coordinate gold atoms. The predicted stretching frequency of 1517 $cm^{-1}$ agrees with a weakly activated dioxygen moiety (cf. $\nu(O{-}O) = 1556.23\ cm^{-1}$),[12] similar to that observed in neutral $Au_4O_2$.[6b] The second oxygen ligand is seen to bind at a two-coordinate site and in so doing causes the first $O_2$ unit to switch from $\eta^1$ to $\eta^2$ binding. This in turn results in a red-shift of the stretching frequency for the $\eta^2$-bound dioxygen. This shift is not predicted to be as strong as observed experimentally, but is still significant from the initial value. This gradual activation is also reflected in the charge transfer analyzed by a natural population analysis, showing a partial charge for $Au_4O_2^+$ on the dioxygen ligand of approximately zero. Upon addition of the second dioxygen, however, the $\eta^2$-coordinated dioxygen becomes charged by −0.15 e. The charge on the $\eta^1$-bound dioxygen, conversely, is zero, reflecting the differing activation of the dioxygen moieties. None of the found stable minima for $Au_4O_2^+$ and $Au_4(O_2)_2^+$ predicted an oxygen vibration which is blue shifted compared to the value of free $O_2$, thus the observed feature at 1720 $cm^{-1}$ is assigned to being a combination of the 1470 $cm^{-1}$ mode and one of the Au-($O_2$) stretching vibrations (predicted to be around 240–300 $cm^{-1}$).

The structure for $Au_{10}O_2^+$ is only slightly distorted from the known bare-metal structure,[17] with the oxygen molecule bound in a $\eta^2$ fashion and a predicted O–O frequency of 1174 $cm^{-1}$, that is, a superoxo moiety. The Au-($O_2$) bond dissociation energy is calculated to be larger for $Au_{10}O_2^+$ than for $Au_4O_2^+$, albeit only slightly (0.1 eV). This is in agreement with the relative mass spectrometric abundances of the complexes being comparable, indicating a similar level of reactivity for these two species. The natural population analysis for the $Au_{10}O_2^+$ cluster shows a greater charging (−0.42 e) of the oxygen moiety than in $Au_4(O_2)_2^+$.

Two modes of interaction are thus observed for the cationic gold clusters with molecular oxygen; in one the first dioxygen ligand reacts to form a superoxo moiety and a doubly charged gold cluster. Such an interaction should be expected to be unfavorable thermodynamically as the ionization energies (IEs) of the cationic gold clusters are high.[18] That this mode of interaction is only observed for $Au_{10}^+$ and $Au_{22}^+$ is attributed to the removal of an electron resulting in a closed-shell within the spherical jellium model containing the "magic" numbers of 8 ($1s^21p^6$) and 20 ($1s^21p^61d^{10}2s^2$) electrons, respectively, lowering the IEs of these clusters. The absence of such binding for $Au_4^+$, which would lead to the "magic" electron count of 2 ($1s^2$), is attributed to the generally higher IEs of the smallest clusters.[19]

The preservation of the jellium shell structure of $Au_{10}^{2+}$ by formation of $Au_{10}O_2^+$ is illustrated in Figure 4. The jellium type or "superatom" orbitals of the eight-electron closed shell system of $Au_{10}^{2+}$, including the LUMO are shown, as well as the mapping of these orbitals onto those of the cluster complex $Au_{10}O_2^+$. The low-lying 1s superatom orbital hybridizes with the low-energy π-bonding orbitals of the dioxygen to form a σ-bonding and anti-bonding orbital pair. The triply degenerate set of orbitals comprising the $1p^6$ electrons of $Au_{10}^{2+}$ have this degeneracy lifted. Two of these orbitals are largely non-bonding in their interaction with the $O_2$ whilst the third points along the axis of the $Au_{10}$-$O_2$ bond and is raised in energy relative to the other two. Energetically the next orbital is a non-bonding orbital centered exclusively on the dioxygen. Finally the LUMO of $Au_{10}^{2+}$ leads to a bonding interaction with the orthogonal π* orbital of $O_2$, and is the HOMO of $Au_{10}O_2^+$.

The alternative interaction instead involves initial physisorption which, at higher coverage, changes to activation. This most likely arises as a result of a solvation induced depression of the second IE. Such a mechanism is supported by the observation that when three Ar atoms are bound to $Au_4^+$, a superoxo mode is observed for the first $O_2$ ligand (Supporting Information, Figure S3). For $Au_{21}^+$ this is somewhat surprising as it is already a "magic" 20 electron cluster. However, removal of two electrons (by formation of two superoxo species) would lead to 18 electrons, corresponding to the closed-shell $1s^21p^61d^{10}$ configuration.

In summary, we have shown that the cationic gold clusters react with molecular oxygen without the aid of a support effect or a co-adsorbate and that these clusters are capable of

  

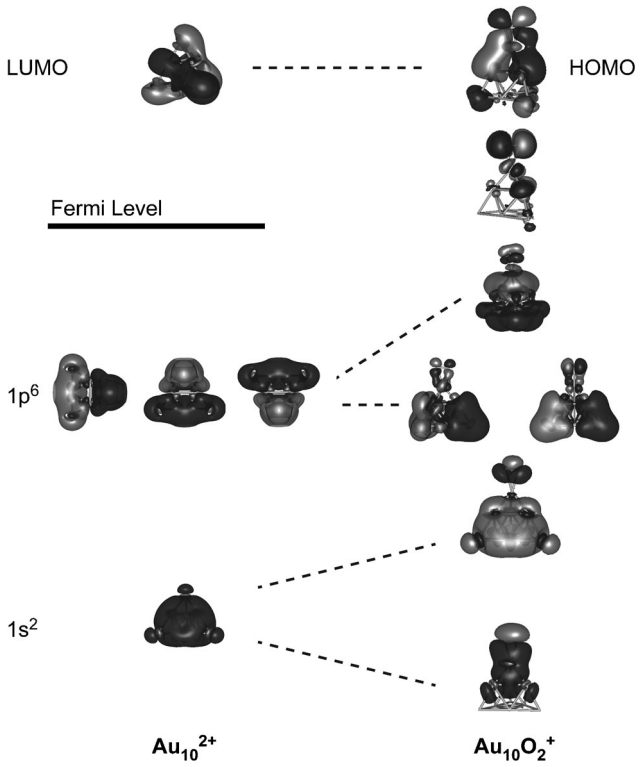


***Figure 4.*** Mapping from the $Au_{10}^{2+}$ superatom orbitals onto the orbitals of the $Au_{10}O_2^{+}$ cluster complex, demonstrating the preservation of the superatom character after the interaction. For $Au_{10}O_2^{+}$ the occupied orbitals of the majority spin states are shown, the minority states are almost identical. The d-type orbitals located at the gold cluster are omitted for clarity.

activating the oxygen molecules towards further reaction through the formation of superoxide moieties. This activation appears linked to the second IE of the corresponding cluster, as species that attain "magic" electron counts spontaneously form the superoxide whereas others require an initial solvation induced depression of the second ionization energy in a self-promoting mechanism.

Received: February 25, 2014
Published online: May 21, 2014

**Keywords:** clusters · gold · nanocatalysis · O-O activation · vibrational spectroscopy

[1] a) M. Haruta, *Cattech* **2002**, *6*, 102–115; b) A. S. K. Hashmi, G. J. Hutchings, *Angew. Chem. Int. Ed.* **2006**, *45*, 7896–7936; *Angew. Chem.* **2006**, *118*, 8064–8105.

[2] a) R. J. Davis, *Science* **2003**, *301*, 926–927; b) T. Risse, S. Shaikhutdinov, N. Nilius, M. Sterrer, H.-J. Freund, *Acc. Chem. Res.* **2008**, *41*, 949–956; c) G. Bond, D. Thompson, *Gold Bull.* **2000**, *33*, 41–50.

[3] I. X. Green, W. Tang, M. Neurock, J. T. Yates, *Science* **2011**, *333*, 736–739.

[4] a) B. Yoon, H. Häkkinen, U. Landman, A. S. Wörz, J.-M. Antonietti, S. Abbet, K. Judai, U. Heiz, *Science* **2005**, *307*, 403–407; b) X. Lin, B. Yang, H.-M. Benia, P. Myrach, M. Yulikov, A. Aumer, M. A. Brown, M. Sterrer, O. Bondarchuk, E. Kieseritzky, J. Rocker, T. Risse, H.-J. Gao, N. Nilius, H.-J. Freund, *J. Am. Chem. Soc.* **2010**, *132*, 7745–7749.

[5] a) J. Guzman, B. C. Gates, *J. Am. Chem. Soc.* **2004**, *126*, 2672–2673; b) J. Guzman, B. C. Gates, *J. Phys. Chem. B* **2002**, *106*, 7659–7665; c) G. Hutchings, M. Hall, A. Carley, P. Landon, B. Solsona, C. Kiely, A. Herzing, M. Makkee, J. Moulijn, A. Overweg, *J. Catal.* **2006**, *242*, 71–81.

[6] a) A. P. Woodham, G. Meijer, A. Fielicke, *Angew. Chem. Int. Ed.* **2012**, *51*, 4444–4447; *Angew. Chem.* **2012**, *124*, 4520–4523; b) A. P. Woodham, G. Meijer, A. Fielicke, *J. Am. Chem. Soc.* **2013**, *135*, 1727–1730; c) W. Huang, H.-J. Zhai, L.-S. Wang, *J. Am. Chem. Soc.* **2010**, *132*, 4344–4351; d) Q. Sun, P. Jena, Y. D. Kim, M. Fischer, G. Ganteför, *J. Chem. Phys.* **2004**, *120*, 6510–6515.

[7] L. D. Socaciu, J. Hagen, T. M. Bernhardt, L. Wöste, U. Heiz, H. Häkkinen, U. Landman, *J. Am. Chem. Soc.* **2003**, *125*, 10437–10445.

[8] a) S. M. Lang, T. M. Bernhardt, *J. Chem. Phys.* **2009**, *131*, 024310; b) S. M. Lang, T. M. Bernhardt, R. N. Barnett, B. Yoon, U. Landman, *J. Am. Chem. Soc.* **2009**, *131*, 8939–8951.

[9] D. M. Cox, R. Brickman, K. Creegan, A. Kaldor, *Z. Phys. D* **1991**, *19*, 353–355.

[10] D. Oepts, A. F. G. van der Meer, P. W. van Amersfoort, *Infrared Phys. Technol.* **1995**, *36*, 297–308.

[11] A. Fielicke, G. von Helden, G. Meijer, D. B. Pedersen, B. Simard, D. M. Rayner, *J. Phys. Chem. B* **2004**, *108*, 14591–14598.

[12] K. P. Huber, G. Herzberg, Constants of Diatomic Molecules NIST Chemistry WebBook, NIST Standard Reference Database Number 69, National Institute of Standards and Technology.

[13] a) R. Pal, L.-M. Wang, Y. Pei, L.-S. Wang, X. C. Zeng, *J. Am. Chem. Soc.* **2012**, *134*, 9438–9445; b) W. Huang, L.-S. Wang, *Phys. Chem. Chem. Phys.* **2009**, *11*, 2663–2667.

[14] B. E. Salisbury, W. T. Wallace, R. L. Whetten, *Chem. Phys.* **2000**, *262*, 131–141.

[15] M. Schmidt, A. Masson, C. Bréchignac, *Phys. Rev. Lett.* **2003**, *91*, 243401.

[16] H.-C. Fang, Z. H. Li, K.-N. Fan, *Phys. Chem. Chem. Phys.* **2011**, *13*, 13358–13369.

[17] S. Gilb, P. Weis, F. Furche, R. Ahlrichs, M. M. Kappes, *J. Chem. Phys.* **2002**, *116*, 4094–4101.

[18] I. Rabin, W. Schulze, *Chem. Phys. Lett.* **1993**, *201*, 265–268.

[19] C. Jackschath, I. Rabin, W. Schulze, *Ber. Bunsen-Ges.* **1992**, *96*, 1200–1204.

  